Self-Organization and Flow of Low-Functionality Telechelic Star Polymers with Varying Attraction

Esmaeel Moghimi,*,†,‡ Iurii Chubak,*,§ Antonia Statt,*,‖ Michael P. Howard,⊥ Dimitra Founta,†,‡ George Polymeropoulos,# Konstantinos Ntetsikas,# Nikos Hadjichristidis,*,# Athanassios Z. Panagiotopoulos,‖ Christos N. Likos,§,○ and Dimitris Vlassopoulos†,‡

†Institute of Electronic Structure and Laser, FORTH, Heraklion 71110, Crete, Greece

‡Department of Materials Science and Technology, University of Crete, Heraklion 71003, Crete, Greece

§Faculty of Physics, University of Vienna, Boltzmanngasse 5, A-1090 Vienna, Austria

‖Department of Chemical and Biological Engineering, Princeton University, Princeton, New Jersey 08544, United States

⊥McKetta Department of Chemical Engineering, University of Texas at Austin, Austin, Texas 78712, United States

#Physical Sciences and Engineering Division, KAUST Catalysis Center, Polymer Synthesis Laboratory, King Abdullah University of Science and Technology (KAUST), Thuwal 23955, Kingdom of Saudi Arabia

○Isaac Newton Institute for Mathematical Sciences, 20 Clarkson Road, Cambridge CB3 0EH, United Kingdom

S *Supporting Information*

ABSTRACT: We combine state-of-the art synthesis, simulations, and physical experiments to explore the tunable, responsive character of telechelic star polymers as models for soft patchy particles. We focus on the simplest possible system: a star comprising three asymmetric block copolymer arms with solvophilic inner and solvophobic outer blocks. Our dilute solution studies reveal the onset of a second slow mode in the intermediate scattering functions as the temperature decreases below the θ-point of the outer block, as well as the size reduction of single stars upon further decreasing temperature. Clusters comprising multiple stars are formed and their average dimensions, akin to the single star size, counterintuitively decrease upon cooling. A similar phenomenology is observed in simulations upon increasing attraction between the outer blocks and is rationalized as a result of the interplay between interstar associations and steric repulsion between the star cores. Since our simulations are able to describe the experimental findings reliably, we can use them with confidence to make predictions at conditions and flow regimes that are inaccessible experimentally. Specifically, we employ simulations to investigate flow properties of the system at high shear rates, revealing shear thinning behavior caused by the breakup of interstar associations under flow. On the other hand, the zero-shear viscosity obtained experimentally exhibits a rather weak activation energy, which increases upon rising star concentration. These findings demonstrate the unusual properties of telechelic star polymers even in the dilute regime. They also offer a powerful toolbox for designing soft patchy particles and exploring their unprecedented responsive properties further on.
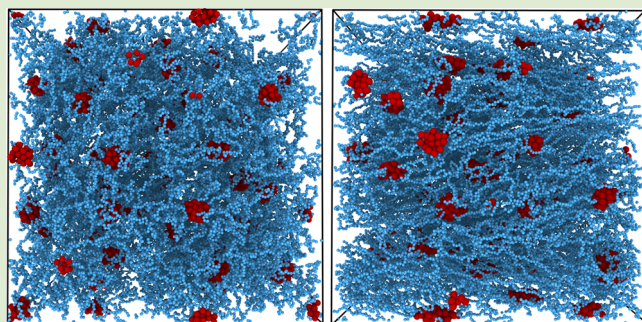
Recently, soft responsive materials have gained a steadily increasing relevance in engineering applications and research because of their functional properties that can be selectively tailored during preparation and via external fields.[1−3] Supramolecular polymeric assemblies are of particular interest in industrial applications because of their outstanding stimuli-responsiveness and their concomitant reversible properties such as self-healing and shape memory.[3−6] In fact, these materials can dramatically change their shape and phase under the influence of external stimuli, for example, temperature, irradiation, pH, electromagnetic fields, or flow.[7−9] Moreover, the use of biologically relevant composites as building blocks of such assemblies opens up a

road for designing novel materials for biomedical or environmental technologies. Single DNA strands serve as a notable example of such programmable units that have been exploited for versatile structure formation.[10−12]

In this work, we present a strategy for developing and investigating well-defined star-shaped block copolymer systems in solvents of varying quality that act as building blocks for supramolecular assemblies using a combination of syntheses, simulations and physical experiments. Given the broad scope
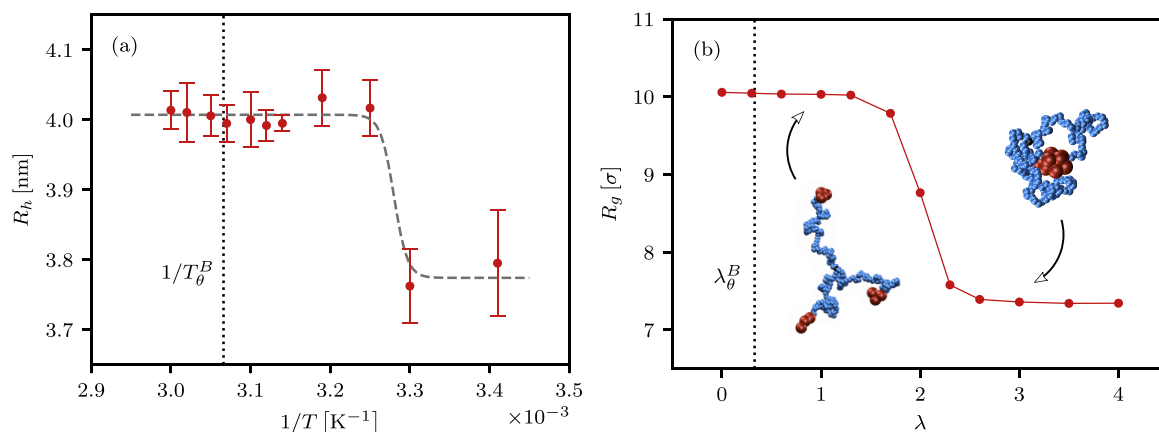
Figure 1. Comparison between single star properties for a star with $f = 3$ arms of $N_A = 65$ and $N_B = 3$, in experiments and simulations. (a) Hydrodynamic radius, R_h, extracted from the fast process in the experimentally determined ISFs at $c = 0.11c^*$. The dashed line is a guide to the eye. (b) Simulated radius of gyration of the same TSP in units of the A-monomer diameter σ as a function of the attraction parameter, λ. Insets illustrate typical conformations of the TSP at corresponding values of λ. Dotted vertical lines in (a) and (b) correspond to the θ-point of the outer block.

and advances in the field of associating polymers,[13,14] we focus on telechelic star polymers (TSPs), which carry associating monomers at their ends.[15−17] A TSP comprises f AB-block copolymers (arms) grafted on a common center with their solvophilic A-blocks being at the interior of the star and their solvophobic B-blocks attached to the end of each arm. In what follows, N_A and N_B denote the number of A- and B-type monomers in a star arm, respectively, and $\alpha = N_B/(N_A + N_B)$ is the relative size ratio between the two block lengths.

The behavior of dilute and concentrated TSP solutions is predominantly governed by the functionality f of the stars, the block size ratio α, and the attraction strength between the solvophobic B-blocks that becomes stronger upon worsening solvent quality. Likewise, structural and viscoelastic properties of melts, in which end-blocks of TSPs associate due to the enthalpic A−B interactions, have been shown to be controlled by the temperature-dependent interplay of intra- and intermolecular associations.[18−21] At infinite dilution, TSPs under such selective solvent conditions form well-defined patches, which allows us to regard them as an experimental realization of soft patchy particles.[16,22−24] Their conformational state-diagram at θ-like conditions for the B-blocks has been set forward in refs 24 and 25 based on simulations of an effective blob model. It has been shown that the patchiness of high functionality TSPs is maintained at finite concentrations and can facilitate the formation of ordered lattices having coordination compatible with the number of patches of a single TSP, suggesting the use of TSPs as tunable building blocks for the formation of multiscale hierarchical supramolecular structures.[4,24−26] In contrast, as shown by means of extensive on-lattice simulations, solvophobic blocks of low functionality TSPs tend to form micellar aggregates[27−30] that can subsequently self-organize at higher concentrations into long wormlike micelles bridged by arms of individual stars.[27,31] Finally, compared to triblock copolymers (i.e., $f = 2$), which tend to self-organize into flower-like micelles that interconnect at higher concentrations,[32,33] star-shaped copolymers have a higher propensity to form intermicellar bridges, as they can split their three arms into three distinct micelles. Therefore, they are expected to have distinct rheological properties.

These predictions have not yet been fully tested, let alone materialized experimentally, in a systematic way that exploits the versatility of TSP structures and properties. In particular, of

prime importance are the exact role of tunable attractions between the outer blocks of TSPs, the corresponding structure formation in concentrated systems, and the associated change of macroscopic properties (such as viscosity) due to microstructural reorganization in flow. In this article, we address these questions to demonstrate the exciting possibilities for designing and fabricating novel materials with tailored rheology.

A well-defined 3-arm star diblock copolymer $(PS\text{-}b\text{-}PB_{1,4})_3$ was synthesized by anionic polymerization and chlorosilane chemistry using high-vacuum techniques in custom-made glass apparatuses. The weight-average total molar mass was $M_{w,LS\text{-}SEC} = 26700$ g/mol, the associated polydispersity was Đ $= 1.03$, and the weight fraction of terminal polystyrene blocks was $f_{PS} = 23\%$ w/w. The stars were dissolved in 1-phenyl dodecane, which is a θ-solvent for the outer PS block[34] with a cloud-point at 53.5 °C and a θ-solvent for the inner PB block at 22 °C. In addition, this solvent has a boiling point of 330 °C at atmospheric pressure and is therefore amenable to rheological experiments. The dynamics of the system were measured by Dynamic Light Scattering (DLS) and the shear viscosity by rheometry. Details about the synthesis and solution preparation, as well as DLS and rheological measurements, can be found in the Supporting Information (SI).

We developed a complementary coarse-grained simulation model for the TSPs based on the Kremer−Grest model[35] for linear polymer chains in a good solvent. Interactions between the A-A and A-B pairs were purely repulsive, mimicking good solvent conditions, while the B−B pairs had a Lennard-Jones-type attraction with a controllable strength λ, which denotes the depth of the potential well[36] and is proportional to an inverse temperature. $\lambda = 0$ is a good solvent, $\lambda = 0.33$ is a θ-solvent for a linear homopolymer, and increasing it decreases the solvent quality. To directly compare with experiments, we simulated 3-arm stars with $N_A = 65$ and $N_B = 3$, which correspond to the number of Kuhn segments in the studied TSP sample (see SI for model details). We note that the employed model aims at capturing essential physical mechanisms at work in associating polymer solutions but not at quantitatively reproducing the specific interactions and dynamics in the experiments.

We first investigated the change of the structure at the single TSP level upon cooling. Figure 1a shows the hydrodynamic
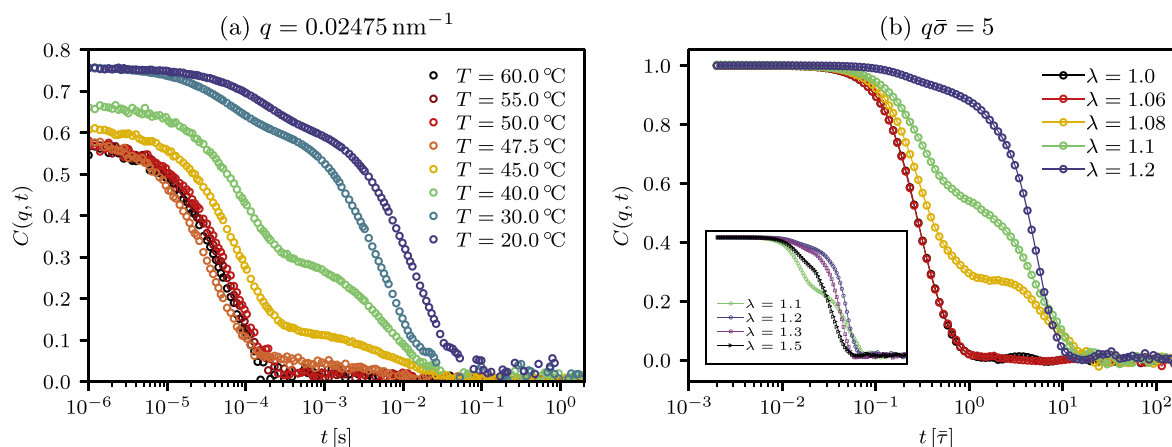
Figure 2. ISFs at different temperatures from (a) experiments and (b) simulations of the coarse-grained blob model at $c = 0.11c^*$. The evolution of a second slow mode is apparent for $T < 47.5$ °C in experiments and for $\lambda > 1.06$ in simulations. Inset in (b) illustrates the decrease of the plateau height corresponding to the second step of the ISF observed in simulations for $\lambda > 1.2$. $\bar{\sigma}$, $\bar{\tau}$ are the length and time units of the blob model simulations (Table S3). The values of experimental $C(q,t)$ smaller than 1 at the lowest t reflect measurement statistics (number fluctuations due to nonconstant number of scatterers in the scattering volume) in these dilute solutions.

radius R_h associated with the fast process in the experimentally measured intermediate scattering functions (ISFs) in the dilute regime and calculated using the Stokes–Einstein–Sutherland relation, which effectively represents the size of a single molecule. As a direct comparison, Figure 1b shows the radius of gyration R_g of the star in units of the A-monomer diameter σ obtained from bead–spring model simulations at different values of λ. Note that the radius of gyration was too small to be probed by DLS; hence, the comparison will be made between experimental R_h and simulated R_g. The former, R_h, is an apparent size of the TSP and it is often assumed that $R_h(T)/R_g(T)$ is a constant ratio; this is not strictly true because of the different origins of these quantities.[37] Nevertheless, the existence of a transition temperature for the single TSP caused by interarm association is an apparent feature of both quantities.

In both cases, we observe reduction of the molecular size upon cooling. Representative snapshots of the TSP given in Figure 1b help to shed light on the self-assembly process that takes place as λ increases for this particular (f, α) combination. When the B-monomers, colored in red, are in a good solvent (i.e., for small values of λ), the star is open and the attraction between star arms is negligible. In this regime, TSPs resemble usual athermal star polymers. Upon worsening the solvent quality, solvophobic monomers first start to form transient patches $(1 < \lambda < 2.5)$ that can be easily destroyed by thermal fluctuations. On further increasing λ, this ultimately leads to the collapse of all three arms of the TSP into one large patch $(\lambda > 2.5)$ accompanied by a significant decrease in R_g.[22] Similarly, R_h of a single TSP reduces upon cooling below $T = 30$ °C. Furthermore, in both cases, the decrease in TSP size occurs within a narrow region of inverse temperature and λ that is notably shifted away from the θ-point of the outer block. Therefore, we argue that cooling (increasing attraction) triggers a similar self-assembly process in both the experiments and simulations. On the other hand, in the experiments we observe only 5% reduction in size, being at the limits of measurement resolution, whereas this reduction amounts to 25% in the simulations. Such a discrepancy is highly plausible to originate from the simulation model, which includes neither details of the atomistic intermolecular interaction that are

relevant for the precise values nor details or possible modifications of the A–A and A–B interactions upon cooling. Nevertheless, it captures the basic physics of self-organization, that is, the end-monomer association. Finally, the different nature of R_h and R_g renders the main value of this comparison qualitative, but even a 5% size reduction can significantly influence properties that depend on the volume fraction in dense systems.

Next, we examine the dynamics of TSPs. To be able to study self-assembly in larger systems and to reach longer time scales, we developed an even coarser simulation model from the bead–spring model by grouping certain segments of a star arm into blobs and subsequently deriving effective potentials between the blobs by means of a rigorous approach that incorporates the many-body correlations that become important at finite densities[38] (see SI for details). Figure 2 shows the ISFs from both experiments and blob model simulations at a fixed wavevector and various temperatures (attraction strengths) for $c = 0.11c^*$, where c^* is the TSP overlap concentration (see SI). The ISF shows two distinct patterns, as seen in Figure 2a. At temperatures above T_θ of the outer block, the ISF exhibits a single exponential decay, demonstrating the existence of freely moving stars in solution. However, upon cooling the system well below T_θ of the outer block $(T < 47.5$ °C in experiments and $\lambda > 1.06$ in simulations), a two-step decay in the ISF is observed. The slow process becomes more pronounced as T is decreased. Identical trends emerge in the ISFs extracted from blob model simulations, as shown in Figure 2b, although the difference between the fast and slow mode relaxation times is an order of magnitude smaller than the one observed experimentally. We attribute this discrepancy to the minimal character of the blob model, which features soft interblob steric potentials and does not take into account hydrodynamic interactions mediated by the solvent, and to the finite box size that limits the growth of the clusters that constitute the slow component of the solution. Furthermore, similar information is recovered when ISFs at various wavevectors are examined: at high $T = 60$ °C or low $\lambda = 1.0$, the ISF shows a single exponential decay at all q-values, whereas at low $T = 40$ °C or high $\lambda = 1.2$, the ISF exhibits a clear two-step decay both in experiments and simulations
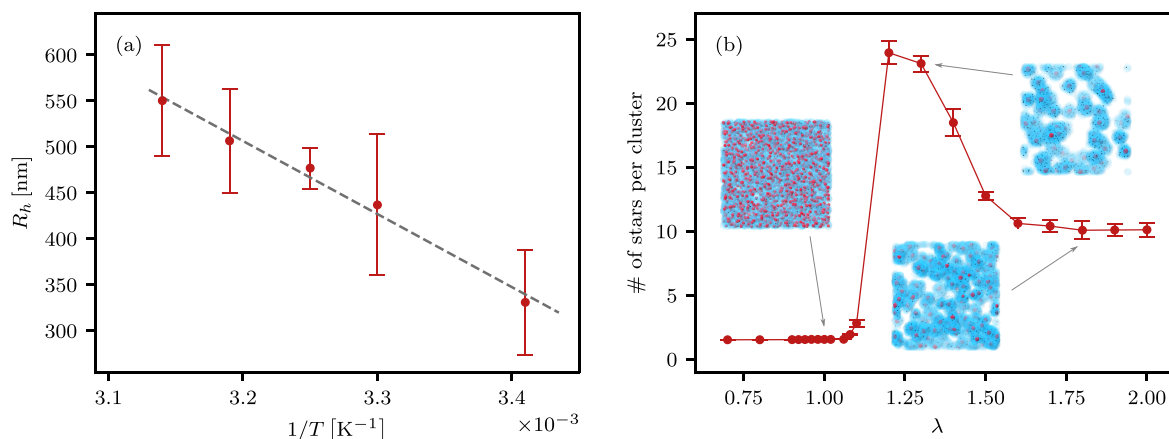
Figure 3. (a) Hydrodynamic radius, R_h, extracted from the slow process in the experimental ISFs. (b) Average aggregate size as a function of λ extracted from simulations of the coarse-grained blob model. Insets: representative configurations of TSPs for indicated λ with the gray arrows (attractive blobs, red; repulsive blobs, light blue; star centers, black). Both results correspond to $c = 0.11c*$.
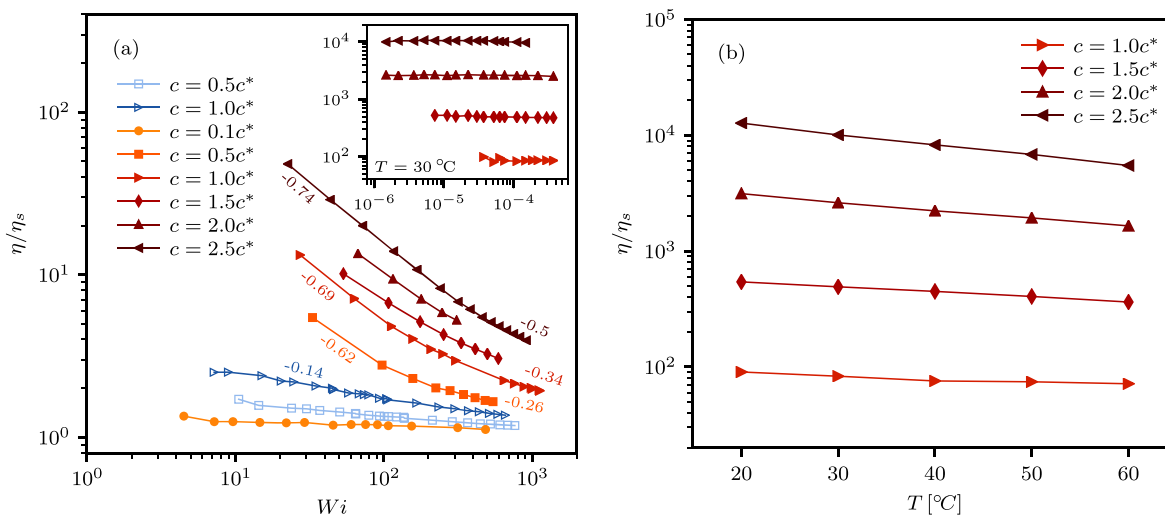
Figure 4. (a) Shear viscosity as a function of Weissenberg number Wi from monomer-resolved simulations obtained at $\lambda = 1$ (open symbols) and $\lambda = 3$ (closed symbols) for various TSPs concentrations. The numbers next to the viscosity curves indicate the slopes of the latter in the corresponding range of Wi. Inset: viscosity data from experiments at $T = 30\ °C$ and low Wi numbers. (b) Temperature dependence of the zero-shear viscosity from experiments at different concentrations, indicating a small activation energy ranging from 20 to 35 kJ/mol for $c/c* = 1-2.5$.

(Figures S8 and S9). Finally, a few characteristic data points available in both the experiments and simulations allow us to establish a relation between λ and $1/T$ (Figure S10 and the associated discussion).

The two-step relaxation of the dynamics indicates the coexistence of clusters (slow process) and single TSPs (fast process). The relaxation spectrum deduced from the inverse Laplace transformation of the ISF using the constraint regularized method[39] reveals two well-separated peaks that represent the relaxation times of single stars and clusters (Figure S4). The corresponding relaxation times are used to calculate the diffusion coefficient and, subsequently, the hydrodynamic radius of a TSP and clusters using the Stokes−Einstein−Sutherland relation. Figure 3a shows R_h corresponding to the slow process. The obtained values exceed the full stretch length of the (PS−PB)$_3$ copolymer, which clearly indicates the formation of the interchain aggregates that decrease in dimensions on cooling.

Simulations provide insights into such change and reveal how the morphology of the TSP network and its rearrangements depend on λ. Figure 3b shows the average cluster size as

a function of λ for $c = 0.11c*$ together with the corresponding simulation snapshots of the TSP structures. At high temperatures ($\lambda < 1.06$), the dynamics of the TSPs are predominantly diffusive: stars occasionally form intra- and intermolecular patches encompassing few arms, which quickly dissociate due to thermal noise. Further cooling ($1.06 < \lambda < 1.2$) dramatically increases aggregation capabilities of a patch: we observe the formation of micelles composed out of attractive B-blocks externally shielded by the inner self-avoiding A-blocks (see Figure 3b). The micelles feature a rather broad size distribution and can be interconnected; that is, there are TSPs whose arms belong to distinct patches, giving rise to clusters (see Figure S7 for characteristic distributions of patch and cluster sizes). Another structural rearrangement of the system occurs by further reducing the temperature ($\lambda > 1.2$): stronger attraction between outer blocks causes tightening of the respective micellar cores, which simultaneously leads to enhanced steric constraints between self-avoiding inner blocks distributed on the exterior of these micelles. Eventually, due to core crowding, some arms or even TSPs leave a micelle, which results in smaller aggregation sizes of patches and clusters and
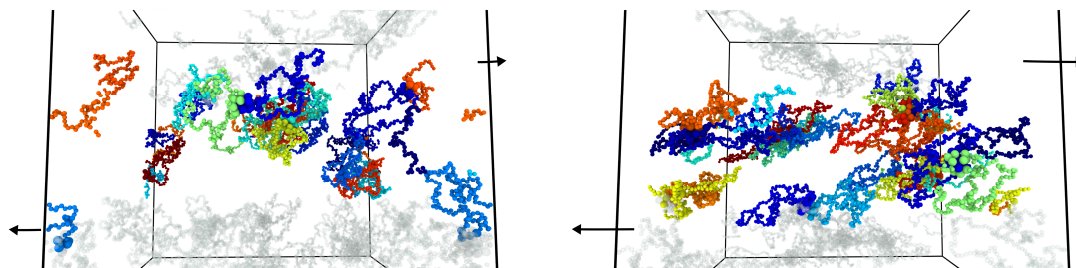
Figure 5. Representative configurations from the bead−spring model simulations of TSPs at $Wi = 14.6$ (left) and $Wi = 107.4$ (right) at $c = 0.1c^*$ and $\lambda = 3$.
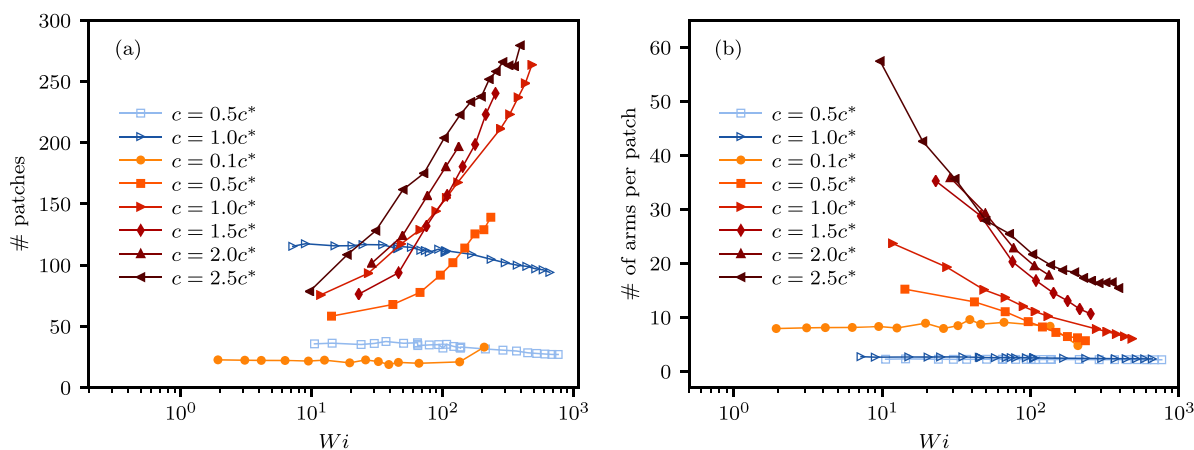
Figure 6. (a) Number of patches and (b) their size as a function of Wi obtained from bead−spring model simulations at $\lambda = 1$ (open symbols) and $\lambda = 3$ (closed symbols) and various concentrations.

decreased intermicellar separation, as seen in the insets of Figure 3b. This reorganization, however, increases micellar interconnectivity, as more stars attach their arms to two or even three distinct patches (see Figure S6 for patch sizes and TSP interconnectivity). This scenario calls for a strong interplay between intra- and interstar association, which is an important design consideration for tailoring the properties of soft patchy particles. We argue that the combined structural and dynamical information from Figures 2 and 3 provides strong evidence about the tunability of TSPs.

Next, we examine the steady state response of TSPs to simple shear flow. We carried out a study combining experiments that probed the system at low shear rates, thereby capturing only the Newtonian regime, and simulations at very high shear rates, where clear shear-thinning behavior was detected. In simulations of the bead−spring model, shear flow was generated by the reverse nonequilibrium simulation method[40] with an explicit solvent modeled by multiparticle collision dynamics[41] in the HOOMD-blue simulation package (modified version 2.3.0).[42−45] The effect of shear flow on TSPs was investigated at $\lambda = 1$ and 3, where the stars are open and collapsed at the single molecule level, respectively, under different concentration regimes.

Figure 4 shows the viscosity measurements from simulations and experiments for TSPs at various shear rates, concentrations, and temperatures. In both cases, the TSP viscosity was normalized by the solvent viscosity, η_s, and the shear rate, $\dot{\gamma}$, was multiplied by the Brownian time of a single TSP, τ_0, to define the Weissenberg number, $Wi = \dot{\gamma}\tau_0$. The results from both experiments and simulations indicate an increase in the relative solution viscosity upon decreasing T (increasing λ). For TSPs with moderate attraction ($\lambda = 1$) at $c \leq c^*$, as well as

for $\lambda = 3$ at $c = 0.1c^*$, we observe a Newtonian regime at small Wi combined with a weak shear-thinning of viscosity at higher Wi with the slope of viscosity, $\eta/\eta_s \sim Wi^{-\delta}, \delta \approx 0.1$ (see Figure 5 for representative TSP conformations). Upon increasing c for the system with higher attraction ($\lambda = 3$), we first detect a transition from a Newtonian to a weakly thinning response, and then to a strongly thinning response. In this case, the slope of viscosity at high Wi is reduced, suggesting a tendency toward an infinite-rate limiting viscosity, which implies saturation of deformation of the inner blocks in shear flow (at $\lambda = 3$ and $c = 2.5c^*$, for example, δ decreases from 0.74 to 0.5 upon rising Wi). This is further confirmed by the fact that TSPs stretch and tend to align their arms along the flow direction (Figure S11). In addition, experimental data for very dilute solutions of linear polymers ($c < 0.2c^*$) indicates very low slopes, similar to that of c^* solution at $\lambda = 1$ in our case, both in good and θ-like solvent conditions. The slope grows with increasing concentration and reaches 0.5 in the semidilute unentangled regime,[46,47] while simulations provide even higher values, up to 0.75.[48,49] Slopes ranging from 0.3 to 0.4 for increasing c have been reported for dilute solutions of star polymers with up to 50 arms in good solvent.[50] The wide range of slopes reflects the complexity of these multiscale TSP systems, which are very different from simple polymers, yet their thinning is associated with deformation of segments and breakup of patches.

As determined by simulations, the microscopic origin of shear-thinning in solutions of TSPs can be qualitatively linked to the fission of patches between outer blocks in shear flow. The dependence of the number and size of patches on Wi are shown in Figure 6a and b, respectively. For $\lambda = 1$, the shear rate had only a small effect on the patches. On average, the patches

contained 2−3 arms and the number of patches decreased slightly with increasing flow rate because the patches were broken up by the rearrangement of the polymers under shear, leaving behind free arms. Such behavior is consistent with the weak shear-thinning of viscosity observed in Figure 4a. On the other hand, for $\lambda = 3$, the patches were broken up into smaller ones under strong shear rates, resulting in a steep increase of their number, and hence implying a strongly thinning response.

In conclusion, we have shown how a simple 3-arm telechelic star polymer, a soft patchy particle, is a paradigm for a designer material with tunable structure and rheology. Tunability is easily achieved by varying the strength of attraction between the associating terminal monomers of the TSP, that is, by selecting a proper solvent that is at the same time good for the inner blocks but poor for the outer ones and then controlling the temperature. We demonstrated this promising possibility in dilute solutions, where such tuning leads to an interplay between intra- and interstar associations that result first in the formation of clusters comprising multiple stars in the system and then to reduction of their size upon cooling. The clusters are gel precursors that can be characterized by a weak flow activation energy, but have substantial deformability in strong shear fields due to the disintegration of interstar patches. The combination of system simplicity and unprecedented richness of material behavior make this approach particularly promising. The satisfactory agreement between experiment and simulations suggests a powerful strategy to design soft responsive patchy particles with tunable macroscopic properties.

■ ASSOCIATED CONTENT

Ⓢ Supporting Information

The Supporting Information is available free of charge on the ACS Publications website at DOI: 10.1021/acsmacro-lett.9b00211.

> Detailed information on the synthesis, sample preparation, DLS, rheological experiments, CONTIN analysis, and instrumentation; bead−spring simulation model; coarse-graining and the resulting blob simulation model; parameters of the explicit solvent and shear flow generation in simulations; additional comparison between ISFs obtained from experiments and simulations; additional information on the structure formation of TSPs in the dilute regime upon cooling and the corresponding distribution of patch and cluster sizes; the relation between λ and T; radius of gyration, sphericity, and anisotropy of TSPs in shear flow (PDF)

■ AUTHOR INFORMATION

Corresponding Authors

*E-mail: esmaeel@iesl.forth.gr.
*E-mail: iurii.chubak@univie.ac.at.
*E-mail: astatt@princeton.edu.
*E-mail: nikolaos.hadjichristidis@kaust.edu.sa.

ORCID Ⓞ

Iurii Chubak: 0000-0003-3042-3146
Michael P. Howard: 0000-0002-9561-4165
George Polymeropoulos: 0000-0002-3352-0948
Konstantinos Ntetsikas: 0000-0002-9236-931X
Nikos Hadjichristidis: 0000-0003-1442-1714
Athanassios Z. Panagiotopoulos: 0000-0002-8152-6615
Christos N. Likos: 0000-0003-3550-4834
Dimitris Vlassopoulos: 0000-0003-0866-1930

Notes

The authors declare no competing financial interest.

■ REFERENCES

(1) Glotzer, S. C.; Solomon, M. J. Anisotropy of Building Blocks and Their Assembly into Complex Structures. *Nat. Mater.* **2007**, *6*, 557−562.

(2) Cloitre, M., Ed. In *High Solid Dispersions*; Springer: Berlin, Germany, 2010.

(3) Cordier, P.; Tournilhac, F.; Soulié-Ziakovic, C.; Leibler, L. Self-Healing and Thermoreversible Rubber from Supramolecular Assembly. *Nature* **2008**, *451*, 977−980.

(4) Bianchi, E.; Capone, B.; Kahl, G.; Likos, C. N. Soft-Patchy Nanoparticles: Modeling and Self-Organization. *Faraday Discuss.* **2015**, *181*, 123−138.

(5) Chakrabarty, R.; Mukherjee, P. S.; Stang, P. J. Supramolecular Coordination: Self-Assembly of Finite Two- and Three-Dimensional Ensembles. *Chem. Rev.* **2011**, *111*, 6810−6918.

(6) Mather, P. T.; Luo, X.; Rousseau, I. A. Shape Memory Polymer Research. *Annu. Rev. Mater. Res.* **2009**, *39*, 445−471.

(7) Wu, Y.; Wang, L.; Zhao, X.; Hou, S.; Guo, B.; Ma, P. X. Self-Healing Supramolecular Bioelastomers with Shape Memory Property as a Multifunctional Platform for Biomedical Applications via Modular Assembly. *Biomaterials* **2016**, *104*, 18−31.

(8) Fameau, A.-L.; Saint-Jalmes, A. Yielding and Flow of Solutions of Thermoresponsive Surfactant Tubes: Tuning Macroscopic Rheology by Supramolecular Assemblies. *Soft Matter* **2014**, *10*, 3622−3632.

(9) Zhuge, F.; Hawke, L. G. D.; Fustin, C.-A.; Gohy, J.-F.; van Ruymbeke, E. Decoding the Linear Viscoelastic Properties of Model Telechelic Metallo-Supramolecular Polymers. *J. Rheol.* **2017**, *61*, 1245−1262.

(10) Xing, Z.; Ness, C.; Frenkel, D.; Eiser, E. Structural and Linear Elastic Properties of DNA Hydrogels by Coarse-Grained Simulation. *Macromolecules* **2019**, *52*, 504−512.

(11) Fernandez-Castanon, J.; Bianchi, S.; Saglimbeni, F.; Di Leonardo, R.; Sciortino, F. Microrheology of DNA Hydrogel Gelling and Melting on Cooling. *Soft Matter* **2018**, *14*, 6431−6438.

(12) Bomboi, F.; Romano, F.; Leo, M.; Fernandez-Castanon, J.; Cerbino, R.; Bellini, T.; Bordi, F.; Filetici, P.; Sciortino, F. Re-entrant DNA Gels. *Nat. Commun.* **2016**, *7*, 13191.

(13) Zhang, Z.; Chen, Q.; Colby, R. H. Dynamics of Associative Polymers. *Soft Matter* **2018**, *14*, 2961−2977.

(14) Winnik, M. A.; Yekta, A. Associative Polymers in Aqueous Solution. *Curr. Opin. Colloid Interface Sci.* **1997**, *2*, 424−436.

(15) Lo Verso, F.; Likos, C. N. End-Functionalized Polymers: Versatile Building Blocks for Soft Materials. *Polymer* **2008**, *49*, 1425−1434.

(16) Pitsikalis, M.; Hadjichristidis, N.; Mays, J. W. Model Mono-, Di-, and Tri-ω-Functionalized Three-Arm Star Polybutadienes. Association Behavior in Dilute Solution by Dynamic Light Scattering and Viscometry. *Macromolecules* **1996**, *29*, 179−184.

(17) Charalabidis, D.; Pitsikalis, M.; Hadjichristidis, N. Model Linear and Star-Shaped Polyisoprenes with Phosphatidylcholine Analogous End-Groups. Synthesis and Association Behavior in Cyclohexane. *Macromol. Chem. Phys.* **2002**, *203*, 2132−2141.

(18) Vlassopoulos, D.; Pakula, T.; Fytas, G.; Pitsikalis, M.; Hadjichristidis, N. Controlling the Self-Assembly and Dynamic

Response of Star Polymers by Selective Telechelic Functionalization. *J. Chem. Phys.* **1999**, *111*, 1760−1764.

(19) Vlassopoulos, D.; Pitsikalis, M.; Hadjichristidis, N. Linear Dynamics of End-Functionalized Polymer Melts: Linear Chains, Stars, and Blends. *Macromolecules* **2000**, *33*, 9740−9746.

(20) Zilman, A. G.; Safran, S. A. Entropically Driven Attraction between Telechelic Brushes. *Eur. Phys. J. E: Soft Matter Biol. Phys.* **2001**, *4*, 467−473.

(21) Van Ruymbeke, E.; Vlassopoulos, D.; Mierzwa, M.; Pakula, T.; Charalabidis, D.; Pitsikalis, M.; Hadjichristidis, N. Rheology and Structure of Entangled Telechelic Linear and Star Polyisoprene Melts. *Macromolecules* **2010**, *43*, 4401−4411.

(22) Lo Verso, F.; Likos, C. N.; Mayer, C.; Löwen, H. Collapse of Telechelic Star Polymers to Watermelon Structures. *Phys. Rev. Lett.* **2006**, *96*, 187802.

(23) Lo Verso, F.; Likos, C. N.; Löwen, H. Computer Simulation of Thermally Sensitive Telechelic Star Polymers. *J. Phys. Chem. C* **2007**, *111*, 15803−15810.

(24) Capone, B.; Coluzza, I.; Lo Verso, F.; Likos, C. N.; Blaak, R. Telechelic Star Polymers as Self-Assembling Units from the Molecular to the Macroscopic Scale. *Phys. Rev. Lett.* **2012**, *109*, 238301.

(25) Capone, B.; Coluzza, I.; Blaak, R.; Verso, F. L.; Likos, C. N. Hierarchical Self-Assembly of Telechelic Star Polymers: from Soft Patchy Particles to Gels and Diamond Crystals. *New J. Phys.* **2013**, *15*, 095002.

(26) Rovigatti, L.; Capone, B.; Likos, C. N. Soft Self-Assembled Nanoparticles with Temperature-Dependent Properties. *Nanoscale* **2016**, *8*, 3288−3295.

(27) Lo Verso, F.; Panagiotopoulos, A. Z.; Likos, C. N. Aggregation Phenomena in Telechelic Star Polymer Solutions. *Phys. Rev. E* **2009**, *79*, 010401.

(28) Lo Verso, F.; Panagiotopoulos, A. Z.; Likos, C. N. Phase Behavior of Low-Functionality, Telechelic Star Block Copolymers. *Faraday Discuss.* **2010**, *144*, 143−157.

(29) Koch, C.; Likos, C. N.; Panagiotopoulos, A. Z.; Lo Verso, F. Self-Assembly Scenarios of Block Copolymer Stars. *Mol. Phys.* **2011**, *109*, 3049−3060.

(30) Koch, C.; Panagiotopoulos, A. Z.; Lo Verso, F.; Likos, C. N. Phase Behavior of Rigid, Amphiphilic Star Polymers. *Soft Matter* **2013**, *9*, 7424−7436.

(31) Koch, C.; Panagiotopoulos, A. Z.; Lo Verso, F.; Likos, C. N. Customizing Wormlike Mesoscale Structures via Self-Assembly of Amphiphilic Star Polymers. *Soft Matter* **2015**, *11*, 3530−3535.

(32) Giacomelli, F. C.; Riegel, I. C.; Petzhold, C. L.; da Silveira, N. P.; Štěpánek, P. Internal Structural Characterization of Triblock Copolymer Micelles with Looped Corona Chains. *Langmuir* **2009**, *25*, 3487−3493.

(33) Giacomelli, F. C.; Riegel, I. C.; Petzhold, C. L.; da Silveira, N. P.; Štěpánek, P. Aggregation Behavior of a New Series of ABA Triblock Copolymers Bearing Short Outer A Blocks in B-Selective Solvent: From Free Chains to Bridged Micelles. *Langmuir* **2009**, *25*, 731−738.

(34) Geerissen, H.; Wolf, B. A. Phenylalkanes as Theta-Solvents for Polystyrene. *Makromol. Chem., Rapid Commun.* **1982**, *3*, 17−21.

(35) Kremer, K.; Grest, G. S. Dynamics of Entangled Linear Polymer Melts: A Molecular-Dynamics Simulation. *J. Chem. Phys.* **1990**, *92*, 5057−5086.

(36) Huissmann, S.; Blaak, R.; Likos, C. N. Star Polymers in Solvents of Varying Quality. *Macromolecules* **2009**, *42*, 2806−2816.

(37) Rubinstein, M.; Colby, R. H. *Polymer Physics*; Oxford University Press: New York, 2003.

(38) Ladanyi, B. M.; Chandler, D. New Type of Cluster Theory for Molecular Fluids: Interaction Site Cluster Expansion. *J. Chem. Phys.* **1975**, *62*, 4308−4324.

(39) Provencher, S. W. CONTIN: A General Purpose Constrained Regularization Program for Inverting Noisy Linear Algebraic and Integral Equations. *Comput. Phys. Commun.* **1982**, *27*, 229−242.

(40) Müller-Plathe, F. Reversing the Perturbation in Nonequilibrium Molecular Dynamics: An Easy Way to Calculate the Shear Viscosity of Fluids. *Phys. Rev. E: Stat. Phys., Plasmas, Fluids, Relat. Interdiscip. Top.* **1999**, *59*, 4894−4898.

(41) Malevanets, A.; Kapral, R. Mesoscopic Model for Solvent Dynamics. *J. Chem. Phys.* **1999**, *110*, 8605−8613.

(42) Howard, M. P.; Panagiotopoulos, A. Z.; Nikoubashman, A. Efficient Mesoscale Hydrodynamics: Multiparticle Collision Dynamics with Massively Parallel GPU Acceleration. *Comput. Phys. Commun.* **2018**, *230*, 10−20.

(43) Glaser, J.; Nguyen, T. D.; Anderson, J. A.; Lui, P.; Spiga, F.; Millan, J. A.; Morse, D. C.; Glotzer, S. C. Strong Scaling of General-Purpose Molecular Dynamics Simulations on GPUs. *Comput. Phys. Commun.* **2015**, *192*, 97−107.

(44) Anderson, J. A.; Lorenz, C. D.; Travesset, A. General Purpose Molecular Dynamics Simulations Fully Implemented on Graphics Processing Units. *J. Comput. Phys.* **2008**, *227*, 5342−5359.

(45) https://github.com/mphoward/azplugins.

(46) Pan, S.; Nguyen, D. A.; Dünweg, B.; Sunthar, P.; Sridhar, T.; Ravi Prakash, J. Shear Thinning in Dilute and Semidilute Solutions of Polystyrene and DNA. *J. Rheol.* **2018**, *62*, 845−867.

(47) Graessley, W. W. *The Entanglement Concept in Polymer Rheology*; Springer Berlin Heidelberg: Berlin, Heidelberg, 1974; pp 1−179.

(48) Larson, R. G. The Rheology of Dilute Solutions of Flexible Polymers: Progress and Problems. *J. Rheol.* **2005**, *49*, 1−70.

(49) Pamies, R.; Lopez Martinez, M. C.; Hernandez Cifre, J. G.; Garcia de la Torre, J. Non-Newtonian Viscosity of Dilute Polymer Solutions. *Macromolecules* **2005**, *38*, 1371−1377.

(50) Singh, S. P.; Chatterji, A.; Gompper, G.; Winkler, R. G. Dynamical and Rheological Properties of Ultrasoft Colloids under Shear Flow. *Macromolecules* **2013**, *46*, 8026−8036.